Absolute cross sections and polarization for electron-impact excitation of the resonance multiplet of the Be$^+$ ion

P. O. Taylor,* R. A. Phaneuf,† and G. H. Dunn‡

Joint Institute for Laboratory Astrophysics, University of Colorado and National Bureau of Standards, Boulder, Colorado 80309

(Received 25 February 1980)

Crossed beams of electrons and ground state Be$^+$ ions have been used to measure absolute cross sections for electron-impact excitation of the 313.1-nm resonance radiation corresponding to the transition Be$^+(2p) \rightarrow$ Be$^+(2s)$. Polarization fractions of the emitted light were also measured. Cross sections are absolute in the sense that all measurables including photon flux at 313 nm have been compared to relevant standards. The doublet emission cross section in units of 10^{-16} cm^2 can be represented as a function of electron energy by $\sigma = -5.10 \ln E + 23.0$ from 4.4 to 21 eV (extrapolating to 16×10^{-16} cm^2 at the 3.96-eV threshold) and by $\sigma = 101 \ln E/E - 151/E$ from 21 to 740 eV. Total uncertainties at a high (approximately 98%) confidence level are about $\pm 10\%$. Coulomb-Born II calculations of Bely overestimate the value at threshold by a factor of 1.7, and a recent Coulomb-Born calculation by Mann is about 10% higher at 740 eV. Two- and five-state close-coupling calculations lie, respectively, 28% and 19% above the measurement at threshold. For energies from 5 to 300 eV the measured polarization fractions can be represented by $P = -0.0708 \ln E + 0.284$ which given $P = 0.19$ at threshold.

I. INTRODUCTION

Cross sections for electron-impact excitation of ions are important in the diagnostics and modeling of nonequilibrium plasmas.[1] Thus, in the last decade, the crossed-charged-beam technique has been used for direct, and often absolute, excitation cross-section measurements on several significant singly charged ions He$^+$,[2-4] Ar$^+$, Kr$^+$,[5] N$_2^+$,[6] Ca$^+$,[7,8] Mg$^+$,[9,10] Ba$^+$,[11-13] Sr$^+$,[10] Hg$^+$,[14,15] and Li$^+$.[16]

On the other hand, while calculations of the important and difficult to measure low-energy cross sections have long been a major challenge and concern of theory, a satisfactory agreement with experiment has not been achieved for singly charged ions. In cases where published close-coupling calculations coexist with experiment (three-state for Ca$^+$,[17] Mg$^+$,[17] and three- and six-state for He$^+$,[18]), the agreement is not good (e.g., ~40% for Ca$^+$); unsophisticated calculations, such as the effective-Gaunt-factor predictor formula,[19] can often lead to similar or better agreement. Experiments indicate that resonances associated with multiply excited states of the electron-ion system can critically influence the cross sections near threshold. Therefore, in order to obtain reliable cross sections one apparently needs more elaborate calculations involving several excited states of the ions and using accurate wave functions. For the multiply charged lithiumlike ions C^{3+} and N^{4+}, on the other hand, excellent agreement between recent absolute measurements[20,21] and theory[22,23] has been obtained.

In this paper we report measurements of absolute cross sections for exciting the $2^2S_{1/2}$-$2^2P_{1/2,3/2}$

resonance doublet in Be$^+$. Polarization fractions of the unresolved resonance radiation at 313.0 and 313.1 nm are also reported. Be$^+$, isoelectronic with Li, is the simplest "one-electron" ion next to He$^+$, and as such should be amenable to calculation of accurate wave functions and cross sections, providing a simpler challenge to theory than more complex ions. In contrast to work on He$^+$ where the emission occurred at 30.4 nm, the detector for the radiation at 313 nm was calibrated, thus affording the opportunity to obtain absolute cross sections. For He$^+$ $1s \rightarrow 2s$, only relative cross sections normalized to Coulomb-Born calculations at high energy were obtained,[4] and cross sections near threshold were then found to disagree by almost a factor of 2 with close-coupling calculations. Finally, a study of Be$^+$ dovetails both with previous work on the other alkaline earths (Mg$^+$, Ca$^+$, Sr$^+$, Ba$^+$—referenced earlier) and with work on the heavier lithiumlike ions C^{3+} and N^{4+}.[20,21]

Results from a number of calculations for excitation of Be$^+$ are shown in Fig. 1. Included are nonunitarized and unitarized Coulomb-Born[24,25] calculations both without exchange (CBI and CBII) and with exchange (CBXI and CBXII), two-state[25] (2CC) and five-state[25,26] (5CC) close-coupling calculations, unitarized distorted-wave polarized orbital[27] (UDWPOII), and the $\bar{g}$ approximation.[19] A preview of the results of this experiment are also sketched in as the dashed curve. The results of the experiment have previously been included in publications[25-27] of other authors giving theoretical results, though they have not been published directly, pending verification of various experimental factors which will be discussed
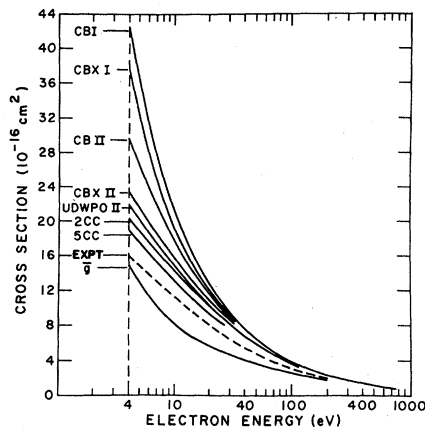
FIG. 1. Cross section (10^{-16} cm^2) versus electron energy (eV) for a number of theories (see text) shown as solid curves, and for the present experiment shown as the dashed curve. Theoretical cross sections are for the excitation Be$^+$(2s) + e → Be$^+$(2p) + e. The experimental curve includes small contributions from cascade, as discussed in Sec. III C. Of two five-state close-coupling calculations, only one is plotted (Ref. 25) to avoid crowding. The other (Ref. 26) includes the effects of pseudostates and lies about 3% lower.

later. The difference between experiment and most complete theory as seen in Fig. 1 is something which the reader will want to keep in mind in studying the details of the experiment which follow.

II. EXPERIMENTAL

The crossed-beam technique and the specific apparatus employed are basically the same as used in the studies of Ca$^+$ excitation; therefore, the Ca$^+$ work[7,28] and a report on the magnetically confined electron source[29] are significant references for the present work.

A collimated ion beam 2.5 mm wide by approximately 6.5 mm high is crossed at right angles with a magnetically confined electron beam 2 mm wide by 10 mm high in a region of ambient pressure about 10^{-7} Pa (i.e., about 7.5×10^{-10} Torr). Photons emitted into a cone along the third orthogonal direction are counted.

The emission cross section σ is extracted from the measured parameters using the equation

$$\sigma = \frac{R}{Y_\Omega I_i I_e} \frac{e^2 v_i v_e}{(v_i^2 + v_e^2)^{1/2}} \frac{\mathfrak{F}}{D(z_0, \lambda)} , \quad (1)$$

where R is the photon signal count rate, e is the electron charge, I_i and I_e are the ion and electron currents, v_i and v_e are the ion and electron velocities, Y_Ω accounts for the anisotropy of the radiation, $\mathfrak{F}$ is the form factor expressing the spatial overlap of the beams and the photodetection rel-

ative sensitivity, and $D(z_0, \lambda)$ is the absolute probability of detecting a photon of wavelength λ emitted in an arbitrary direction from the $z = z_0$ plane inside the collision volume.

Detailed formulas for Y_Ω and $\mathfrak{F}$ and techniques used for measuring the quantities in Eq. (1) are given in the above references. Further discussion will be limited to the features peculiar to this work.

A. Electron source, ion source, and beam modulation

The magnetically confined electron source, tests for spiraling of the electrons, and measurements of energy and energy spread have been described in detail.[28,29] A small modification to the electron collector to eliminate secondary electrons has been noted[13] in work on Ba$^+$. The source delivered currents from 0.02 mA at 4 eV to (for example) 1.5 mA at 250 eV.

A simple, commercial, hot-filament, discharge-ion source[30] was used to produce Be$^+$ ions. Chips of Be metal were placed in the discharge crucible and a discharge struck with CCl$_4$ which, reacting with the Be, provided a source of more volatile BeCl$_4$ for ionization. Ions were extracted from a 0.5-mm hole in the molybdenum anode, mass analyzed, focused, and collimated in the usual way into a 2.5×6.5-mm^2 beam carrying 0.1 μA of ^{9}Be$^+$.

To separate the electron-ion impact signal from various background photon signals, a beam modulation scheme similar to that described by Dance et al.[2,31,32] was used. Normal signal count rates during cross-section measurements ranged from 1 to 25 sec^{-1}, and the background rate ranged from 8 to 240 sec^{-1} as the energy was varied from 4 to 240 eV.

B. Photon detection and optical calibration

Absolute measurement of light fluxes encountered in crossed-beam excitation is difficult and may be a likely target for suspicion when the accuracy of the measured cross section is under discussion. Hence, in this section we provide a moderately detailed description of the optical detection and calibration procedure.

To measure a photon flux at 313 nm a detection system with quartz optics was used and techniques were developed for extending the previously applied[7,28] optical calibration procedure into the near uv. Photons passing through a 2.54-cm aperture, representing an f/1.59 solid angle, were collimated by a pair of planoconvex lenses made of ultraviolet-quality fused silica, selected by an interference filter (12 nm FWHM), and converged by another short-focal-length quartz lens onto the

1-cm-diameter photomultiplier cathode. The multiplier, of the same quartz-windowed red-insensitive type as previously investigated and used,[7] was incorporated in a commercial housing, and when cooled to -25°C produced a dark count of about 1 sec^{-1}.

Routine pulse-height analysis showed a stable pulse transmission through the pulse amplifier-discriminator circuitry of about 97%. Measured dead time of the counting system was $\tau_D=0.56$ ±0.07 μsec, necessitating small corrections to some count rates encountered during calibration.

Relative sensitivity of the photomultiplier tube (PMT) was monitored and normalized with a stable β^- emission-excited scintillator. During the course of calibration and cross-section measurements (4months) the PMT showed fluctuations and drifts of about $\pm2\%$, which were corrected for with an assessed uncertainty of $\pm1\%$.

A rotatable uv polarizing sheet could be inserted to measure the degree of polarization P of the light relative to the electron-beam axis. The measured polarizance of the sheet was $K=0.9885$ (K is defined by $P=P_{observed}/K$). The fractional polarization contributed by the detection system minus polaroid was $P=0\pm0.005$. Automatic 90° rotation of the polarizer between short-photon-flux counting periods allowed us to obtain accurate polarization measurements despite the low uv transmission (ca. 18%) of the polaroid.

As in the previous work a "monochromatic" light source of the same area as the beam intersection area was used to determine $D(z_0,\lambda)$ in Eq. (1). The source was realized by passing light from either a 200-W quartz-iodide (QI) lamp, or a small Hg discharge lamp, through a 35-cm grating monochromator set for 0.25-nm bandpass. The selected light was coupled via a fused silica light pipe with high uv transmittance into a 10-mm-i.d. integrating sphere with a 2×1.5-mm^2 rectangular exit aperture. Detailed measurements on the source showed it to be uniform, non-polarized, and isotropic over the viewing space of the detector.

The calibration transfer was performed by first comparing the "transfer source" to a standard of spectral radiance using a spectroradiometer. The latter consisted of a grating monochromator, lens preoptics, an interference filter for additional rejection of scattered light, and a cooled photomultiplier. The transfer source was then inserted directly into the collision volume at height z_0, and the photon flux was measured to determine $D(z_0,\lambda)$.

Quartz-lens preoptics were used for the spectroradiometer, and the position and size of the "target" (i.e., image of the monochromator en-

trance slit formed by the preoptics lens) were measured as a function of wavelength. Thus it could be ensured that the target was always coincident with the plane of the source and contained within it. The size of source effect[33-35] (which exists because the amount of light refracted and scattered into the radiometer entrance slit from outside the target depends on the extent of the source) was measured and found to require a correction of 0.34$\pm0.02\%$ when comparing the transfer source to the larger-area blackbody standard sources.

A vacuum copper-point (1357.8 K) blackbody designed in this laboratory was used as a primary standard to calibrate the sensitivity of the spectroradiometer at various wavelengths above 390 nm. Intercomparisons made in this laboratory show our vacuum cooper-point blackbody to be 1.6% brighter at 455 nm than an evacuated tungsten strip lamp calibrated for radiance against the National Bureau of Standards (NBS) gold-point blackbody standard.[37] As a standard at shorter wavelengths the spectral radiance of a vacuum tungsten strip lamp was adjusted to correspond to that of a 1357.8-K, or alternatively a 1650-K blackbody, at one of those wavelengths; the spectral radiance at shorter wavelengths was then deduced from a relationship[38] which involved only the wavelengths, the reported spectral emissivities of tungsten,[39] and measured lamp-window transmissions at each wavelength. Use of the strip lamp at the higher temperature facilitated the uv calibration by providing more source intensity (the response to the 1357.8-K source was only 1.1 sec^{-1} at 313 nm). The low count rates encountered during uv intercomparisons made it advantageous to employ a chopper wheel of measured duty cycle to allow accurate subtraction of dark count. Because of the remaining difference between experiment and theory already mentioned in discussing Fig.1, it was supposed that one of the main targets of suspicion from the experimental viewpoint was the spectral radiance standard. Thus,[40] a high-temperature ($\sim$2650-K) strip lamp was calibrated by the National Bureau of Standards (NBS) and compared with the standard (1650 K) used in the experiment. The comparison showed the experimental standard to be accurate within 1.5%, assuming the NBS calibrated lamp to be exact (the quoted NBS uncertainty at 313 nm is 2%).

One can show that the relationship between the sensitivity $D(z_0,\lambda)$ and the quantities measured in the transfer intercomparison is

$$D(z_0,\lambda_m)=\frac{1}{4\pi A_\Omega}\frac{C_S(\lambda_M)}{L_S(\lambda_M)}\frac{C_F(z_0,\lambda_M)}{C_C(\lambda_M)}\frac{I_C}{I_S I_F}. \qquad (2)$$

Here A_Ω is the average projected area of the trans-

fer source as seen by the collision apparatus detector through its solid angle Ω, and $C_F(z_0, \lambda_M)$ is the count rate observed with the transfer source in the apparatus at height z_0 and coincident with the crossed-beam intersection. $C_C(\lambda_M)$ is the count rate when the spectroradiometer views the transfer source, $C_S(\lambda_M)$ is the count rate when the radiometer views the standard source of radiance $L_S(\lambda_M)$, and the quantities I_F, I_S, and I_C are given by

$$ I_F(\lambda_M) = \int_0^\infty W_R(\lambda)t(\lambda, \lambda_M)D_R(z, \lambda)d\lambda \,, $$

$$ I_S(\lambda_M) = \int_0^\infty L_{SR}(\lambda)R_R(\lambda)s(\lambda, \lambda_M)d\lambda \,, $$

$$ I_C(\lambda_M) = \int_0^\infty W_R(\lambda)R_R(\lambda)t(\lambda, \lambda_M)s(\lambda, \lambda_M)d\lambda \,. $$

In these last equations the subscript R denotes that the function gives the variation in wavelength relative to unity at $\lambda = \lambda_M$. The functions $t(\lambda, \lambda_M)$ and $s(\lambda, \lambda_M)$ are the normalized slit functions of the transfer-source monochromator and spectroradiometer monochromator, respectively. $W(\lambda)$ is the spectral radiance of the transfer source (including the monochromator, light pipe, and integrating sphere), and $R(\lambda)$ is the effective spectral response of the spectroradiometer.

When the transfer source is used with the QI lamp the integrals I_C, I_S, and I_F (which relate to the bandpasses of, and scattered light effects in, the monochromators) are evaluated from measured functions as described previously.[7] However, the Hg lamp line spectrum included an emission at 313.17 nm and, for calibration at this and certain other shorter wavelengths, provided a more-intense transfer light source. For this line source the integrals $I_C = I_F = 1$ [since $W(\lambda)$ is a delta function at $\lambda = \lambda_M$], and the comparison of the two techniques at all possible wavelengths provides a stringent test on the transfer procedure. All radiance intercomparisons could be done without resorting to use of superfluous neutral-density filters, *in situ* transmissions of which can be difficult to ascertain.

The variations of sensitivity with position in the interaction volume, needed to calculate $\mathfrak{F}$ in Eq. (1), were obtained at $\lambda = 313$ nm by measuring the detection-system response to a diffuse isotropic light source as the source was spatially scanned in the collision volume. This source was similar to the transfer light source with Hg discharge lamp, but used a more flexible light pipe and terminus.

The entire transfer procedure, performed at several wavelengths, was repeated twice for each source and averages were taken after a small

correction for lamp power and PMT sensitivity drift (using a scintillator source as monitor). Final analysis of the data gave $D(z_0, 313.1) = 4.05 \times 10^{-4}$ ($\pm 7\%$) counts per photon evaluated from the QI transfer source and $D(z_0, 313.17) = 4.01 \times 10^{-4}$ ($\pm 6\%$) evaluated from the Hg source. The average of the two calibrations was used: $D(z_0, 313.1) = 4.03 \times 10^{-4}$ ($\pm 5\%$) counts/photon. The uncertainties here are total uncertainties at a high confidence level, as explained below.

C. Uncertainties

Systematic uncertainties have been evaluated in separate experiments, or assessed from analysis of the data, or from previous experience with the apparatus. Where sufficient experimental data on the systematic effects were available we have expressed the associated uncertainty at the same 98% confidence level (98% CL) applied to all the random uncertainties (typically three standard deviations of the mean). In other cases we have assessed the uncertainty at a high confidence level (HCL) which we feel is comparable with the 98% CL. The total uncertainty is obtained by first taking the direct sum of possibly correlated uncertainties, and then combining this in quadrature with uncorrelated uncertainties. We label uncertainties obtained in this way by HCL, thus reserving the term 98% CL as a statement of confidence limits on statistically evaluated uncertainties.

Table I lists the significant sources of uncertainty in evaluating the absolute photon-detection sensitivity at 313 nm using the QI transfer source. The total quadrature uncertainty in this absolute calibration is 7% (HCL) and the direct sum of all the significant uncertainties is 20%. Use of the more intense Hg lamp transfer source enabled us to obtain better statistics in measuring the response C_C and also reduced the radiometric integral uncertainty to 0.9%. Thus the total quadrature uncertainty in this case was 6%.

Table II lists all the uncertainties in the cross-section measurements at an energy of 5 eV excluding those associated with absolute optical calibration. Each cross-section datum point represents at least a 1000-sec integration period resulting in a statistical (Poisson) standard deviation of 1.6 to 4.6%. Thus the statistical uncertainty at 98% CL ranged from 5 to 14% with an average of 7.5%. The data were obtained from stepwise scans of the electron energy, but the beam overlap factor was not measured at every energy. Thus the 2% (HCL) uncertainty in the form-factor measurement $\mathfrak{F}$ includes allowance for energy and time interpolations. An additional uncertainty of 1% in $\mathfrak{F}$ is associated with the small (<1%) correction for the distances the excited ions travel

TABLE I. Significant sources of uncertainty in evaluating the absolute photon-detection sensitivity at 313 nm. Uncertainties are expressed at a high confidence level (HCL) as explained in the text (Sec. II C). Values are for the calibration transfer using the quartz-iodide source. Use of the more intense Hg lamp source reduced the uncertainty in C_C (to 1%) and in $I_C/I_S I_F$ (to 0.9%), so in this case the total quadrature uncertainty was 5.8%.

Source of uncertainty	Percentage uncertainty	
	Direct sum	Quadrature
Projected source area A_Ω	0.8	0.6
Calculated strip-lamp radiance $L_S(313)$:		
Copper point (±0.4 K SD)	3.0	3.9
Emissivity of W and transmission of quartz	2.5	
Setting of and response to strip lamp $C_S(313)$:		
Blackbody response reproducibility (above 390 nm)	1.2	
Strip-lamp response reproducibility (at 313 nm)	2	2.5
PMT sensitivity normalization	1	
Transfer factor C_F/C_C:		
Reproducibility of C_F	0.85	
Reproducibility of C_C	1.7	
PMT sensitivity normalization in C_F	1	
PMT sensitivity normalization in C_C	1	3.6
Setting of wavelength λ_M	1	
Rotation correction and light-pipe stability	1	
Nonuniformity and anisotropy of emitting area	1	
Position of emitting area in collision volume	2	
Radiometric integrals $I_C/I_S I_F$	3.8	3.8
Total uncertainty in $D(z_0, 313)$	20	7.0

TABLE II. Significant sources of uncertainty in the relative emission cross-section measurements at an energy of 5 eV. Uncertainties are expressed at a high confidence level (HCL) as explained in the text (Sec. II C).

Source of uncertainty	Percentage uncertainty	
	Direct sum	Quadrature
Counting statistics (98% CL)	7.5	7.8
Form-factor measurement $\mathcal{F}$	2	
Path-length correction	2	4
Anisotropy correction	2	
Uncollected electron current	0.2	
Electron-current calibration	0.5	
Ion-current calibration	0.5	
Ion-beam horizontal position	1.5	2.4
Ion velocity	1	
Finite lifetime correction in $\mathcal{F}$	1	
PMT sensitivity normalization	1	
Combined uncertainty in $\sigma(E)$		
excluding absolute optical calibration	19	9

before radiating. The anisotropy correction depends on the electron path length as well as polarization, and hence is combined linearly with the path-length correction. The sum of these uncertainties is 4% (HCL) at 5 eV but rapidly decreases to less than 1% at 100 eV. Since all the uncertainties listed in Table II, including ion velocity and current calibration, can depend on energy or on time of data taking, the combined uncertainty shown in this table represents the point-to-point relative uncertainty of the cross-section data. For much of the data this relative uncertainty was less than 9% and actually ranged from 5.5 to 14% (HCL). Combining the relative uncertainty with the uncertainty of 6% in $D(z_0, 313$ nm) leads to a total quadrature HCL uncertainty in the absolute cross-section data ranging from 8 to 15% (typically 10%).

III. RESULTS

A. Polarization

The linear polarizations of the combined multiplet emission at 313.0 and 313.1 nm are presented in Fig. 2 as a function of incident electron energy. Since the ions are sufficiently slow to be considered stationary relative to even the lowest electron speed, the polarization fraction has been evaluated as $P_0 = (I_\parallel - I_\perp)/(I_\parallel + I_\perp)$, where $I_\parallel$ and $I_\perp$ are normalized count rates observed with the polaroid axis, respectively, parallel and perpendicular to the electron-beam axis. Small corrections have been applied at each energy for polar-
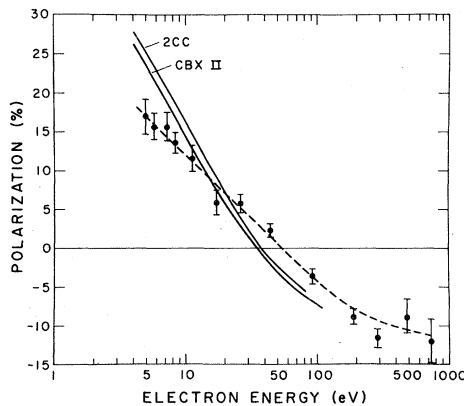
FIG. 2. Linear polarizations of the combined multiplet emission at 313.0 and 313.1 nm resulting from electron-impact excitation of the $2p$ level of Be$^+$. Points represent present measurements; uncertainties are standard deviations combined in quadrature with systematic uncertainties. Curves are calculated using two-state close-coupling (2CC) and unitarized Coulomb-Born calculations with exchange (CBXII) approximations (Ref. 25).

izance of the polaroid ($P_1 = P_0/0.989$), finite solid angle $\{P_2 = P_1/[1 - 0.0255(1 - P_1)]$ for $f/1.59$ optics$\}$, and dilution due to spiraling electron trajectories $\{P = P_2/[1 - (\Delta L/L_0)(3 - P_2)]\}$, where $\Delta L/L_0$ is the fractional path-length increase$\}$ (see Ref. 7 for details.) At all energies the major source of uncertainty was statistical, and the flags on Fig. 2 represent one standard deviation derived from counting statistics combined in quadrature with systematic uncertainties.

The measured polarization shows qualitatively the form expected from momentum-transfer considerations[41-43]: being positive near threshold, going to zero at about 14 times the threshold energy, and proceeding to negative polarization at high energies. For energies from 5 to 300 eV the measured polarization of the multiplet can be represented by

$$P = -0.0708 \ln E + 0.284 , \qquad (3)$$

which gives the extrapolated value of $P = 0.19$ at the 3.96-eV threshold. Multiplet polarizations calculated in the close-coupling (2CC) and Coulomb-Born (CBXII) approximations,[25] plotted in Fig. 2 for comparison, overestimate the experimental values by about 40% near threshold, and fall below the measurements above 30 eV. The crossover through zero occurs at 36 eV rather than the experimental figure of 55 eV. The long counting times necessitated by small signals precluded a search for structure in the polarization which might be expected in the first 5 eV above threshold.[13, 43]

Since ^{9}Be has a nuclear spin of $\frac{3}{2}$ the Percival and Seaton formula[41] for polarization of $2p$-$2s$ multiplets (which ignores fine structure) gives $P_\infty = -0.069$ as the high-energy limit of the polarization. The measured polarization is already -0.08 at 200 eV, indicating that the effect of fine structure is significant and must be allowed for.[42] The polarization of the $P_{1/2} \rightarrow S_{1/2}$ transition should be zero and the polarization for the $P_{3/2} \rightarrow S_{1/2}$ transition is greater than in Fig. 2 and can be obtained from the measured multiplet polarization P using the formula[28] $P_{3/2} = 9P/(6 + P)$.

B. Cross-section results

Absolute emission cross sections for the 313-nm doublet are presented as a function of incident electron energy by the points in Fig. 3. The data were obtained from four scans of the cross section from below threshold to about 17 eV with a fine energy grid and two scans from 15 to 740 eV with a coarser grid.

Several small corrections have been applied to data calculated from Eq. (1). Obvious corrections are associated with duty cycle of the counter
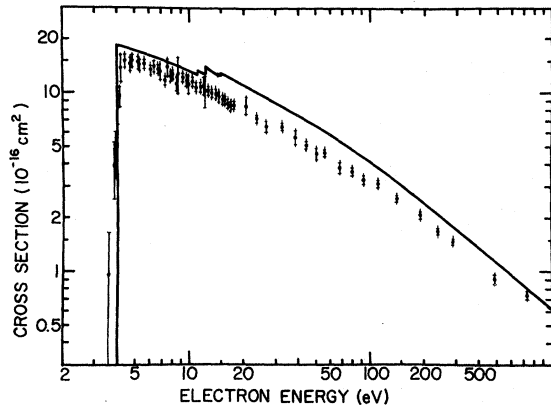
FIG. 3. Log-log plot of cross section in 10^{-16} cm^2 versus electron energy in eV for emission of 313-nm radiation from electron impact on Be$^+$. Points are measurements from this work. Flags depict total uncertainty at a high confidence level (see text). Bars across flags show random uncertainties at the 3σ or 98% CL. The solid theoretical curve is constructed from Eq. (6) using close-coupling cross sections from Ref. 25 for the resonance level and Coulomb-Born cross sections from Ref. 44 for cascade levels.

($\pm 0.2\%$ uncertainty), ion- and electron-current integrator calibration, and light-detection sensitivity fluctuations as monitored by the scintillator light source (the latter corrects for drifts of $< \pm 1\%$ in the pulse transmission of the electronics as well as drifts of $\pm 2\%$ in PMT efficiency). The anisotropy factor in Eq. (1) includes allowance for light collection over a finite solid angle Ω and was corrected for angles introduced by spiraling electron trajectories. Finally, cross sections from Eq. (1) have been divided by $1 + \Delta L/L_0$ because of path-length increases due to spiraling (again see Ref. 7 for details).

The energy scale is corrected for space-charge depression and cathode-contact potential according to the empirical formula given in Ref. 7. It is well known that the cross section for ion excitation is finite at threshold[19]; the slower onset of excitation seen in Fig. 3 is characteristic of the finite energy spread of about 0.4 eV in the electron beam. Thus, for the excitation function plotted in Fig. 3, the point at the "middle" of the linear onset represents the threshold energy within ± 0.1 eV and is used to establish the contact potential for the present oxide cathode.

The flags in Fig. 3 depict total uncertainty (random, systematic, and absolute) at a high confidence level. Bars across the flags show random uncertainty only at 98% CL. Measurements were made verifying that cross sections were independent, within counting statistics of 1 to 2%, of beam modulation frequency and duty cycle,

horizontal ion-beam position, electron current, and residual gas pressure.

The data in Fig. 3 can be represented by

$$\sigma = -5.10 \ln E + 23.0, \quad 4.4 < E < 21 \text{ eV} \qquad (4)$$

$$\sigma = 101 \frac{\ln E}{E} - \frac{151}{E}, \quad 21 < E < 740 \text{ eV}. \qquad (5)$$

The uncertainty in σ computed from these formulas is just the experimental uncertainty, which is about $\pm 10\%$ (HCL) at most energies. We present these least-squares fit formulas for numerical reference rather than tabulate the 86 points represented in Fig. 3. Equation (4) extrapolates to give a threshold emission cross section of 16 $\times 10^{-16}$ cm^2.

C. Discussion of results

The measured 313-nm doublet emission cross section is related to the cross section for excitation of the $2p$ doublet by

$$\sigma_{em}(2p \rightarrow 2s) = \sigma_{ex}(2s \rightarrow 2p)$$

$$+ \sum \gamma(nl \rightarrow 2p)\sigma_{ex}(2s \rightarrow nl), \qquad (6)$$

where the sum is over levels higher than $2p$ and the γ's are branching ratios to the $2p$ levels (second-order cascade is ignored). The excitation thresholds for the $n = 3$ levels are near 12 eV, and for the $n = 4$ levels are just below 15 eV.

For comparison of measurement with theory, one must either make separate measurements of $\sigma_{ex}(2s \rightarrow nl)$ and subtract appropriately to obtain $\sigma_{ex}(2s \rightarrow 2p)$, or construct the theoretical $\sigma_{em}(2p \rightarrow 2s)$. The latter course is chosen, since no separate measurements were made of $\sigma_{ex}(2s \rightarrow nl)$. A number of theoretical calculations of $\sigma_{ex}(2s \rightarrow 2p)$ have already been discussed and shown in Fig. 1. The solid curve in Fig. 3 is $\sigma_{em}(2p \rightarrow 2s)$, constructed according to Eq. (6), where $\sigma_{ex}(2s \rightarrow 2p)$ is represented by the close-coupling results of Hayes et al.[25] to 70 eV, and by unitarized Coulomb-Born calculations with exchange[25] (CBXII) to higher energies. Calculations of Mann[44] using CBXII are taken for the cross sections for excitation to the 3^2S, 3^2D, 4^2S, and 4^2D levels, and no higher states were included. Bely[24,25] has also calculated the cross sections for cascading transitions using the CBI approximation, and his results are in agreement with Mann's to within about 10%. Bely makes calculations up to $n = 7$, but inclusion of $n > 4$ would only change the curve in Fig. 3 by about 0.8%. The contribution from the cascade term in Eq. (6) is about 13% at 20 eV and decreases to about 6% at 1000 eV.

One notes that the recent close-coupling results of Henry and van Wyngaarden,[26] in which they in-

clude effects of pseudostates, are a few percent (~3%) lower than those of Hayes *et al.*[25] and may have been more appropriate calculations to use in constructing $\sigma_{em}(2p \rightarrow 2s)$.

As seen in Fig. 1 the various theoretical methods seem to yield results which agree with one another at high energies and which tend to the experimental values as the sophistication of the calculation is increased. However, as seen in Fig. 3, there apparently remains a substantial (15%) disagreement between theory and experiment. In fact, if the experimental curve is uniformly adjusted upwards by 15%, one obtains near-perfect agreement, which suggests a possible 15% systematic error in the experiment. As already noted in Sec. II and Ref. 40, however, the search for one or more systematic errors large enough to support this simplistic interpretation of the disparity between experiment and theory has caused substantial delay in the publication of the results presented here while a careful reevaluation of systematic errors was under way. As we stated earlier, the radiometric standard was thought to be most suspect but has been shown to be accurate[40] to within 1.5%. Indeed, after due consideration, we feel that all sources of error have been accounted for, that the uncertainties in Fig. 3 and Tables I and II are realistic, and that the disparity between theory and experiment cannot be explained so simplistically.

We emphasize that neither the polarization nor cross-section data agree with theory, as is brought out in Figs. 1–3. The discussion below, however, shows that the experimental polarizations and cross sections are consistent with each other.

It is well known[46-48] that at sufficiently high energy the cross section for electron-impact excitation of state j from state i can be represented by the Bethe approximation

$$\sigma_{ij} = \frac{4\pi a_0^2}{E/R} \frac{f_{ij}}{(E_j - E_i)/R} \ln(E/E_0) \qquad (7)$$

for states i and j, which are dipole connected with an oscillator strength f_{ij}. Here $E_j - E_i$ is the energy between levels, $R = 13.605$ eV, a_0 is the Bohr radius, and E_0 is a constant.

McFarlane[49] has shown that in the Bethe approximation the polarization can be given by

$$P = \frac{P_0[3 - \ln(E/E_0)]}{[(2 - P_0)\ln(E/E_0) + P_0]}, \qquad (8)$$

where P_0 is a constant containing the angular information of the atomic transition. Heddle[50] has pointed out that from Eq. (8), one can use experimental measurements of the energy at which polarization is zero to determine E_0, i.e., the polarization goes to zero at $E = e^3 E_0$. He showed the
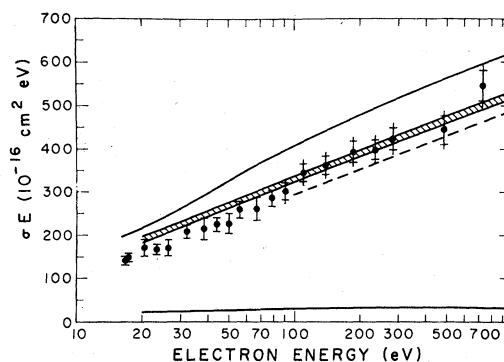
FIG. 4. Collision strength versus log electron energy for excitation of Be$^+$ to give 313-nm radiation. Points are present measurements with flags and bars described in Fig. 3. The upper solid curve is the same as in Fig. 3. The solid curve across the bottom is cascade contribution only. Dashed curve is from $\bar{g}$ approximation, Eq. (9), with cascade added. Solid curves connected with hatching are results from Eq. (7) with E_0 obtained from the intercept of experimental polarization with the energy axis in Fig. 2 [see Eq. (8)]. The two curves result from extreme intercepts possible from the experimental data.

experimental consistency between cross-section measurements and polarization "zero crossings" for a number of cases, including measurements on Ca$^+$ and Ba$^+$ made in this laboratory.[7, 13]

Consider now the collision strength, which for an initial S state is just $\Omega = \sigma E$. For the present case, this quantity is shown plotted against the logarithm of the energy (a so-called Bethe or Fano plot) in Fig. 4. One notes from Eq. (7) that at high enough energies one should obtain a straight line with slope proportional to f_{ij} and with an intercept with the energy axis at E_0. In the figure the experimental points for $E > 16$ eV are shown with cross bars representing relative uncertainties only at 98% CL. The solid curve at the top is $\sigma_{em}(2p \rightarrow 2S)E$, with σ_{em} constructed as outlined above and as shown by the solid curve in Fig. 3. The solid curve across the bottom is the cascade contribution to σ_{em} [the second term on the right side of Eq. (6)]. The two lines with hatching between them are plots of Eq. (7) using extreme values of E_0 obtained from the polarization data in Fig. 2, with[51] $f_{ij} = 0.505$ and with cascade (the solid curve at the bottom) added. Shown as the dashed line in Fig. 4 is the $\bar{g}$ or "effective-Gaunt-factor" approximation[19, 52] with cascade added. This results from the $\bar{g}$ formula

$$\sigma_{ij} = \frac{8\pi}{\sqrt{3}} \frac{\pi a_0^2}{E/R} \frac{f_{ij}}{(E_j - E_i)/R} \bar{g} . \qquad (9)$$

At the high energies for which the curve is plotted in Fig. 4, the recommendation[52] is

$$\bar{g} = (\sqrt{3}/2\pi)\ln[E/(E_j - E_i)],$$

so that Eq. (9) just becomes Eq. (7) with $E_0 = E_j - E_i$. The simple $\bar{g}$ approximation is, in fact, in better agreement with experiment than any of the theoretical calculations.

One sees from Fig. 4 that the relationship between the experimental cross sections and polarizations is entirely consistent with that predicted by the Bethe approximation; while again we note that the experimental values of both polarization and cross sections are different from theory. This is not to imply that such consistency is known to be necessary—or even expected, since the Bethe approximation formula for polarization, Eq. (8), may not be applicable at the energies involved (~50 eV). However, as already emphasized, Heddle has shown similar experimental consistency in a number of cases. We further point out that the theory involved in this Be^+ problem is not consistent in this fashion; i.e., collision strengths constructed from Eq. (7) with E_0 derived from the zero crossings of the theoretical polarizations lie in a band roughly halfway between the top theory curve in Fig. 4 and the band resulting from use of experimental polarization zero crossings.

IV. CONCLUSIONS

The disagreement between measured cross sections and polarizations found in this work and theoretical values appears to be large enough for concern. We have carefully examined possible sources of systematic error in the measurements and judged that the uncertainties are assessed conservatively, i.e., that they really are "high confidence uncertainties." This adds to the emerging picture noted in the Introduction that in no case for singly charged ions does theory give cross sections which are in satisfactory agreement with measurements. This contrasts with the multiply charged ions C^{3+} and N^{4+} where experiment and theory agree.

ACKNOWLEDGMENTS

*Present address: Center for Astrophysics, 60 Garden Street, Cambridge, Mass. 02138.

†Present address: Physics Division, ORNL, Oak Ridge, Tenn. 37830.

‡Quantum Physics Division, National Bureau of Standards.

[1]M. J. Seaton, Adv. At. Mol. Phys. 11, 83 (1975).

[2]D. F. Dance, M. F. A. Harrison, and A. C. H. Smith, Proc. R. Soc. London Ser. A 290, 74 (1966).

[3]A. I. Dashchenko et al., Zh. Eksp. Teor. Fiz. 67, 503 (1974) [Sov. Phys.—JETP 40, 249 (1975)].

[4]K. T. Dolder and B. Peart, J. Phys. B 6, 2415 (1973).

[5]I. P. Zapesochnyi et al., Zh. Eksp. Teor. Fiz. 63, 2000 (1972) [Sov. Phys.—JETP 36, 1056 (1973)].

[6]D. H. Crandall, W. E. Kauppila, R. A. Phaneuf, P. O. Taylor, and G. H. Dunn, Phys. Rev. A 9, 2545 (1974).

[7]P. O. Taylor and G. H. Dunn, Phys. Rev. A 8, 2304 (1973).

[8]V. A. Kelman and A. I. Imre, Opt. Spektrosk. 38, 1226 (1975) [Opt. Spectrosc. (USSR) 38, 709 (1975)].

[9]V. A. Kelman, A. I. Daschenko, P. Zapesochnyi, and A. I. Imre, Dokl. Akad. Nauk SSSR 220, 65 (1975) [Sov. Phys. Dokl. 20, 38 (1975)].

[10]I. P. Zapesochnyi et al., in Electronic and Atomic Collisions, Abstracts of Papers of the 9th ICPEAC Conference, edited by J. S. Risley and R. Geballe (University of Washington Press, Seattle, 1975), p. 393.

[11]F. M. Bacon and J. W. Hooper, Phys. Rev. 178, 182 (1969).

[12]M. O. Pace and J. W. Hooper, Phys. Rev. A 7, 2033 (1973).

[13]D. H. Crandall, P. O. Taylor, and G. H. Dunn, Phys. Rev. A 10, 141 (1974).

[14]D. H. Crandall, R. A. Phaneuf, and G. H. Dunn, Phys. Rev. A 11, 1223 (1975).

[15]R. A. Phaneuf, P. O. Taylor, and G. H. Dunn, Phys. Rev. A 14, 2021 (1978).

[16]W. T. Rogers, J. Ø. Olsen, and G. H. Dunn, Phys. Rev. A 18, 1353 (1978).

[17]P. G. Burke and D. L. Moores, J. Phys. B 1, 575 (1968).

[18]P. G. Burke and A. J. Taylor, J. Phys. B 2, 44 (1969).

[19]M. J. Seaton, in Atomic and Molecular Processes, edited by D. R. Bates (Academic, New York, 1962), p. 374.

[20]P. O. Taylor, D. Gregory, G. H. Dunn, R. A. Phaneuf, and D. H. Crandall, Phys. Rev. Lett. 39, 1256 (1977).

[21]D. Gregory, G. H. Dunn, R. A. Phaneuf, and D. H. Crandall, Phys. Rev. A 20, 410 (1979).

[22]N. H. Magee, Jr., J. B. Mann, A. L. Merts, and W. D. Robb, Los Alamos Scientific Laboratory Report No. LA-6691-MS, 1977 (unpublished).

[23]W. L. van Wyngaarden and R. J. W. Henry, J. Phys. B 9, 1461 (1976).

[24]O. Bely, Proc. Phys. Soc. London 88, 587 (1966).

[25]M. A. Hayes, D. W. Norcross, J. B. Mann, and W. D. Robb, J. Phys. B 10, L429 (1977).

[26]R. J. W. Henry and W. L. van Wyngaarden, Phys. Rev. A 17, 798 (1978).

[27]J. V. Kennedy, V. P. Myerscough, and M. R. C. McDowell, J. Phys. B 11, 1303 (1978).

[28]P. O. Taylor, Ph.D. thesis, University of Colorado, 1972 (unpublished; available through University Microfilms Inc.).

[29]P. O. Taylor, K. T. Dolder, W. E. Kauppila, and G. H. Dunn, Rev, Sci. Instrum. 45, 538 (1974).

[30]M. Menzinger and L. Wahlin, Rev. Sci. Instrum. 40, 102 (1969).

[31]Circuitry for the more sophisticated beam-modulation scheme was developed after it was discovered that the previously used scheme (Ref. 11) was inadequate to reliably separate signal from background at less than 1 in 10^3 level which was encountered in the measurement of some very small cross sections (Ref. 15). The scheme employs a 2-MHz (or other) clock with countdown logic circuits to develop the pulse trains for modulating the electron and ion beams and for gating the two scalers. Included in the scheme are refinements (Refs. 2, 32) for averaging any irregularities across the current pulses of between scalers and other refinements for shortening the scaler duty cycle to avoid counting while beams are switching. The signal is obtained by subtracting the counts registered by the two scalers after sufficient time has elapsed to produce the desired statistical precision, and the signal can be separated from a background 10^4 larger.

[32]L. Molyneux, K. T. Dolder, and B. Peart, J. Phys. E 4, 149 (1971).

[33]R. D. Lee, Metrologia 2, 150 (1966).

[34]J. H. Kostkowski, D. E. Erminy, and A. T. Hattenburg, Adv. Geophys. 14, 111 (1970).

[35]T. P. Jones and J. Tapping, Metrologia 8, 4 (1972).

[36]B. Van Zyl and G. H. Dunn (private communication).

[37]This difference must be viewed as small in the light of difficulties associated with guaranteeing identical geometry and current when using strip lamps.

[38]H. J. Kostkowski, Appl. Opt. 5, 1959 (1966).

[39]R. D. Larrabee, J. Opt. Soc. Am. 49, 619 (1959).

[40]The Be⁺ excitation experiment was quoted by others in the literature (Refs. 25–27), but the experimental results were not submitted for publication due to a concern about possible unknown or undetected errors in the 1650-K strip-lamp calibration at 313 nm. Therefore a comparison to the NBS-calibrated high-temperature lamp was performed. Since the radiances agree to 1.5%, well within the estimated uncertainty of the comparison, no adjustments have been made to the data represented in Refs. 25–27. Refer to NBS Test No. 534/C-3.

[41]I. C. Percival and M. J. Seaton, Philos. Trans. R. Soc. London A 251, 113 (1958).

[42]D. R. Flower and M. J. Seaton, Proc. Phys. Soc. London 91, 59 (1967).

[43]U. Fano and J. H. Macek, Rev. Mod. Phys. 45, 553 (1973).

[44]J. Mann (private communication).

[45]O. Bely, Ann. Astrophys. 29, 683, 131 (1966).

[46]S. Geltman, Topics in Atomic Collision Theory (Academic, New York, 1969), Chap. 14.

[47]H. Bethe, Ann. Phys. (Leipzig) 5, 325 (1930).

[48]M. Inokuti, Y. Itikawa, and J. E. Turner, Rev. Mod. Phys. 50, 23 (1978).

[49]S. C. McFarlane, J. Phys. B 7, 1756 (1974).

[50]D. W. O. Heddle, J. Phys. B 12, 489 (1979).

[51]G. A. Martin and W. L. Weise, Phys. Rev. A 13, 699 (1976).

[52]H. Van Regemorter, Astrophys. J. 136, 906 (1962).